

Noncytopathic bovine viral diarrhea virus 2 impairs virus control in a mouse model

Giyong Seong¹ · Jin-Sol Lee¹ · Kyung-Hyun Lee² · Seung-Uk Shin¹ · Ji Young Yoon³ · Kyoung-Seong Choi¹

Received: 13 May 2015 / Accepted: 28 October 2015 / Published online: 19 November 2015
© Springer-Verlag Wien 2015

Abstract Bovine viral diarrhea virus (BVDV) is an economically important pathogen that causes development of mild to severe clinical signs in wild and domesticated ruminants. We previously showed that mice could be infected by BVDV. In the present study, we infected mice intraperitoneally with non-cytopathic (ncp) BVDV1 or ncp BVDV2, harvested the blood and organs of the infected mice at days 4, 7, 10 and 14 postinfection (pi), and performed immunohistochemical analyses to confirm BVDV infection. Viral antigens were detected in the spleens of all infected mice from days 4 through 14 and were also found in the mesenteric lymph nodes, gut-associated lymphoid tissue (GALT), heart, kidney, intestine, and bronchus-associated lymphoid tissue (BALT) of some infected mice. In ncp BVDV2-infected mice, flow cytometric analysis revealed markedly fewer CD4⁺ and CD8⁺ T lymphocytes and lower expression of costimulatory molecules CD80 (B7-1) and CD86 (B7-2) and major histocompatibility complex (MHC) class II (I-A/I-E) than those in ncp BVDV1-infected mice. Production of the cytokines interleukin (IL)-6 and monocyte chemotactic protein (MCP)-1 was higher in the plasma of ncp BVDV2-infected mice than that in that of ncp BVDV1-infected mice. Our results

demonstrate that ncp BVDV1 and ncp BVDV2 interact differently with the host innate immune response *in vivo*. These findings highlight an important distinction between ncp BVDV1 and ncp BVDV2 and suggest that ncp BVDV2 impairs the host's ability to control the infection and enhances virus dissemination.

Introduction

Bovine viral diarrhea virus (BVDV) is one of the most important viral pathogens that can seriously affect cattle productivity, resulting in substantial economic losses in the livestock industry globally. BVDV is classified into two distinct species: *bovine viral diarrhea virus 1* and *bovine viral diarrhea virus 2*. Both these species include viruses of two biotypes: cytopathic (cp) and non-cytopathic (ncp), which differ in their ability to induce cytopathogenic effects in cultured cells [1, 2]. Clinical symptoms of BVDV include diarrhea, respiratory disease, reproductive failure such as abortion, weak calf syndrome, teratogenic effects on fetuses, hemorrhagic syndrome, and mucosal diseases [3–7]. BVDV can induce lymphopenia at the peak of infection, which leads to immunosuppression and can increase susceptibility to secondary bacterial or viral infections [8, 9]. While ncp BVDV1 causes mild to sub-clinical diseases, ncp BVDV2 is associated with clinically severe acute manifestations [10].

Previous studies performed by our group using the same two strains used in the present study showed that calves inoculated intranasally with ncp BVDV2 developed more severe clinical signs, including elevated body temperature, cough, nasal discharge, anorexia, diarrhea, and hematological abnormalities, such as lymphopenia and

G. Seong, J.-S. Lee and K.-H. Lee contributed equally to this work.

✉ Kyoung-Seong Choi
kschoi3@knu.ac.kr

¹ College of Ecology and Environmental Science, Kyungpook National University, Sangju 742-711, Republic of Korea

² Animal Disease Diagnostic Division, Animal and Plant Quarantine Agency, Anyang 430-824, Republic of Korea

³ Jeonju Biomaterials Institute, Jeonju 561-360, Republic of Korea

thrombocytopenia, than those inoculated with ncp BVDV1. The clinical symptoms in ncp BVDV2-inoculated calves lasted longer than those in ncp BVDV1-inoculated ones [11]. Several studies have shown that cattle infected with the highly virulent ncp BVDV2 had decreased levels of costimulatory molecules and antigen presentation [12, 13]. *In vitro* ncp BVDV1 infection increased the levels of IL-12 mRNA at 1 h postinfection, with no effect at 24 h [14]. Infection *in vivo* with ncp BVDV resulted in reduced T-lymphocytes in lymphoid tissues, depending on the strain [15, 16]. ncp BVDV strains may spread within herds and cause secondary infections or severe disease.

Our recent study demonstrated the potential of mice as a model for BVDV infection by intraperitoneal (IP) injection [17], although none of the IP-injected mice in that study exhibited any signs of illness. In a mouse experiment using both ncp BVDV1 and ncp BVDV2, which were the same strains that were used in calves, significant differences were observed between the two strains in histopathological examinations. The histopathological changes in ncp BVDV2-infected mice were moderate to severe compared to those in ncp BVDV1-infected mice [17]. Recently, our group infected mice with cp BVDV via oral inoculation. In contrast to IP injection, oral inoculation led to the development of thrombocytopenia, lymphopenia, and anorexia, which usually occur in cattle, and increased megakaryocytes in the spleen and bone marrow [18]. These results suggest that mice can possibly be used as a host for BVDV infection. Because BVDV causes significant problems in the livestock industry, small animal models may serve as a useful tool for the study of BVDV pathogenesis. Therefore, to better understand the pathogenesis and the events occurring at the time of infection with two ncp BVDV strains in the mouse model of BVDV, we investigated the immunological differences between ncp BVDV1 and ncp BVDV2 infections with respect to the production of important cytokines. The results of the present study provide new evidence for BVDV immunopathogenic mechanisms and show the differences in virulence between two ncp BVDV strains.

Materials and methods

Experimental animals, BVDV culture, and infection of mice

Specific pathogen-free BALB/c mice (6–8 weeks old) were purchased from the Daehan Experimental Animal Center (Daejeon, Korea). All animals were maintained under pathogen-free conditions and handled in strict accordance with the guidelines and protocols approved for these

experiments by the Kyungpook National University Animal Care and Use Committee.

The BVDV1 (472) and BVDV2 (001) strains used in this study were isolated in the Republic of Korea [11] and kindly supplied by Dr. JK Oem, Animal and Plant Quarantine Agency. The preparations of two virus strains were obtained after 5 days of culturing with one freeze-thawing cycle and centrifugation at 3,000 rpm for 10 min to remove large cellular debris. The supernatant was then frozen in -80°C in aliquots until used for inoculation of mice. Each virus was titrated in Madin-Darby bovine kidney (MDBK) cell cultures, and the TCID₅₀ was calculated as described [19].

Four mice inoculated with each BVDV strain and four mock-inoculated mice were sacrificed on days 4, 7, 10, and 14 post-inoculation (pi). Challenge was performed by IP injection of 0.4 mL of culture medium containing 5×10^5 TCID₅₀ of each virus. Mock-infected mice were injected IP with 0.4 mL of the tissue culture medium (minimum essential medium; Life Technologies Corp.; Carlsbad, CA, USA). All experiments were performed twice to confirm reproducibility.

Immunohistochemistry

At each time point, twelve mice for each BVDV strain or mock inoculation were euthanized with CO₂ gas and necropsied for harvesting of tissues on days 4, 7, 10, and 14 pi. For BVDV antigen detection, immunohistochemical staining was performed on formalin-fixed paraffin-embedded blocks of mouse tissues, including tissues of the spleen, liver, kidney, lung, mesenteric lymph nodes, intestine, gut-associated lymphoid tissue (GALT), and bronchus-associated lymphoid tissue (BALT). Briefly, 5- μm -thick paraffin-embedded tissue sections were deparaffinized in xylene, hydrated through a graded alcohol series, and then washed in distilled water. To enhance antigen retrieval, the tissue sections were soaked in heat-induced sodium citrate buffer (pH 6.0) for 30 min, cooled to the room temperature, and then incubated with 3 % H₂O₂ in methanol for 10 min to block the endogenous peroxidase activity. After blocking, samples were treated with primary antibodies according to the manufacturers' protocols. The following antibodies were used: anti-BVDV antibody (Ab) 15C5 (Syracuse Bioanalytical; Ithaca, NY, USA), CD4 (Abcam, Cambridge, UK), CD8a (eBioscience, Inc., San Diego, CA, USA), and CD45R (BD Bioscience, San Jose, CA, USA). After reacting with the primary antibody, the tissue sections were stained with biotinylated anti-mouse IgG (Vector Laboratories, Inc.; Burlingame, CA, USA) for 1 h at room temperature, washed, and incubated with the VECTASTAIN ABC Reagent (Vector) for 30 min. After washing, sections were reacted with

peroxidase substrate solution (Vector), rinsed, counterstained, mounted, and photographed. Negative control slides were prepared with isotype-matched IgG at the same dilution as that used for the primary antibody.

CAIA-based quantification of CD4 and CD8

Immunostained (CD4 and CD8) whole-slide sections were scanned on an iScan Coreo Au Slide Scanner (Ventana Medical Systems, Tucson, AZ, USA), which was kindly provided by Ventana on a loan basis. Scans were saved as BIF files. Semiautomated computer-assisted image analysis (CAIA) was performed with Virtuoso software (Ventana). For each case, a slide was identified and marked for further analysis by a trained histopathologist. Next, the Virtuoso free-hand drawing tool was used to define user-defined regions of interest (ROIs) by gradually increasing the area of the center of the spleen. This was done as follows: the ROI set was placed in the center of the marked spleen, and its size was adjusted to include an arrangement of 15,000 to 20,000 cells. Then, each immunostained (CD4 and CD8) slide was assessed for each cell type by the proprietary Virtuoso Ki67 algorithm (Ventana). The performance of Virtuoso, to determine the correct classification of false-positive cells, was carefully reviewed by two histopathologists via inspection of the quantification overlays at 200× magnification on the computer screen. Observers were advised to reject CAIA results in any case of potentially significant misclassification. The second histopathologist also reviewed the proper selection of ROIs that were selected by the first operator. Cases that were concordantly approved by both observers were included for further analysis.

Flow cytometry for immunophenotyping

The spleens from individual mice (six mice at each time) were minced and dispersed to obtain single-cell suspensions. The cells were washed and lysed in RBC lysis buffer (Sigma, St Louis, MO, USA) to remove erythrocytes, and the remaining cells were then washed and resuspended in PBS. The single cell suspensions were stained with APC-labeled anti-mouse CD3 ϵ (BD), FITC-labeled anti-mouse CD4 (BD), PerCP-labeled anti-mouse CD8 (BD), and PE-labeled anti-mouse CD49b (DX5 α ; BD) in one tube, and with FITC-labeled anti-mouse CD19 (BD), APC-labeled anti-mouse CD80 (B7-1; BD), PerCP-labeled anti-mouse CD86 (B7-2; BD), and PE-labeled anti-mouse MHC class II (I-A/I-E; BD) in another tube, at 4 °C for 15 min. The stained cells were washed twice with PBS containing 0.5 % bovine serum albumin (BSA; Sigma), fixed with 1 % paraformaldehyde (Sigma), and examined by flow cytometry using a FACS Calibur flow cytometer (BD). The

data were analyzed using the FlowJo software (Tree Star, Inc., Ashland, OR, USA), and the gates were set based on the isotype-matched control antibodies.

Plasma cytokine analysis

Cytokines and chemokines in the plasma of ncp BVDV1- or ncp BVDV2-infected mice or mock-infected mice were detected separately at each time point by using a mouse CBA inflammation kit (BD) according to the manufacturer's instructions. Data were acquired on a FACS Calibur flow cytometer (BD). A total of 300 bead events for each cytokine were collected. Analysis of the CBA data was performed using the FCAP Array 3.0 software (Soft Flow, St. Louis, MO, USA).

Statistical analysis

Data are expressed as mean \pm standard error of the mean (S.E.M). Each value was the result of two independent experiments. Statistical analyses were performed by a two-way analysis of variance (ANOVA) using GraphPad Prism V6.0 software (Graphpad Software Inc., San Diego, CA, USA). *P* values < 0.05 were considered significant.

Results

BVDV infection in mice

Mice were infected with BVDV via IP injection. As expected, none of the mice exhibited any clinical signs of illness. The distribution of viral antigens in different organs of the infected mice is summarized in Table 1. No BVDV antigen was detected in any of the tissue samples from the mock-infected mice. IHC results revealed differences in the detection of viral antigen depending on the time of infection (Table 1). Viral antigens were detected in the spleen of all infected mice from days 4 through 14 pi. In addition, viral antigens were detected in the mesenteric lymph nodes, gut-associated lymphoid tissue (GALT), heart, kidney, intestine, and bronchus-associated lymphoid tissue (BALT) of some of the infected mice. Viral antigens in ncp BVDV1-infected mice appeared to be more abundant in the lymphoid tissues at days 4 and 10 pi than in ncp BVDV2 infection (Table 1). Interestingly, viral antigens were detected in the heart and kidney at day 4 pi; they disappeared until day 10, and were detected again at day 14. However, at day 14, the viral antigens were found only in the heart tissue of two mice and the kidney tissue of four mice (Table 1). These viral antigens were detected in the lymphocytes of the spleen, mesenteric lymph nodes, GALT, and BALT. Viral antigens were also detected in the

Table 1 Distribution of BVDV-specific antigen from days 4 through 14 post-inoculation for four mice infected with each BVDV strain

Tissue	Days							
	Day 4		Day 7		Day 10		Day 14	
	Ncp BVDV1	Ncp BVDV2	Ncp BVDV1	Ncp BVDV2	Ncp BVDV1	Ncp BVDV2	Ncp BVDV1	Ncp BVDV2
Heart	4/4	4/4	0/4	0/4	0/4	0/4	0/4	2/4
GALT	2/4	0/4	0/4	2/4	0/4	0/4	0/4	0/4
Mesenteric lymph node	2/4	0/4	0/4	0/4	4/4	0/4	0/4	0/4
Spleen	4/4	4/4	4/4	4/4	4/4	4/4	4/4	4/4
Kidney	4/4	4/4	0/4	0/4	0/4	0/4	2/4	2/4
Intestine	0/4	1/4	0/4	0/4	0/4	0/4	1/4	0/4
BALT	0/4	0/4	0/4	0/4	2/4	0/4	0/4	0/4

GALT, gut-associated lymphoid tissue; BALT, bronchus-associated lymphoid tissue

BVDV antigen was not detected in mock-infected mice

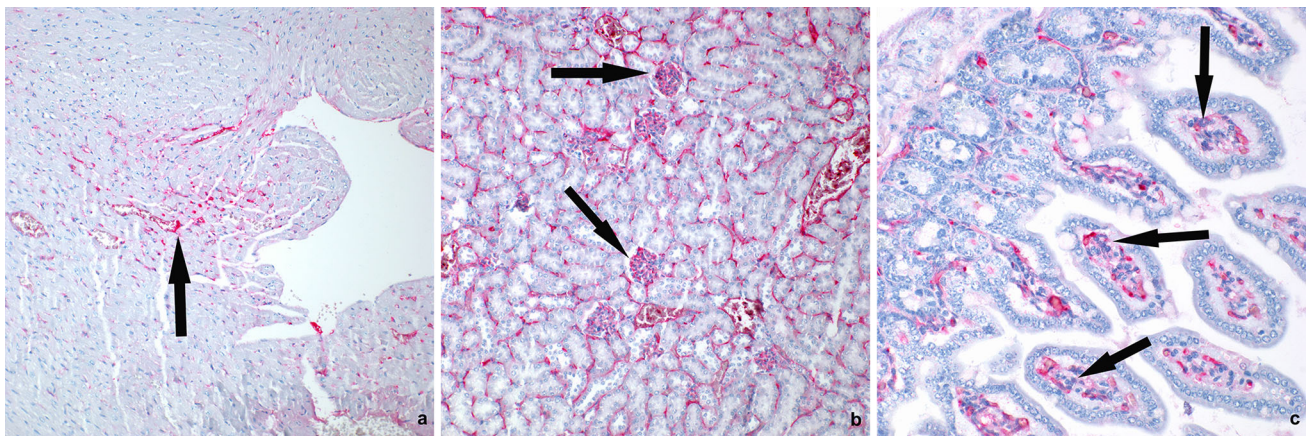


Fig. 1 Immunohistochemistry for BVDV antigen at day 4 after intraperitoneal injection. Viral antigens were detected in the podocytes of glomeruli in the kidney (a), in the myocytes of the heart (b), and in the lamina propria of the intestine (c) (original magnification, 200 \times)

podocytes of the glomeruli in the kidney (Fig. 1a), in the myocytes of the heart (Fig. 1b), and in the lamina propria of the intestine (Fig. 1c). These results suggest that the spleen is the most reliable target organ for detection of BVDV infection.

CD4, CD8, CD19, and co-stimulatory molecule expression on splenocytes following BVDV infection

Flow cytometric analysis revealed that the relative proportions of B and T lymphocytes and the expression of costimulatory molecules (CD80 and CD86) and MHC class II on splenic lymphocytes differed considerably between the BVDV-infected groups (Fig. 2). Compared with that in the mock-infected mice, in ncp BVDV1-infected animals, CD4⁺ T cell populations peaked at day 7 pi and gradually declined at day 14 pi (Fig. 2a), and their cell populations were larger than that in ncp BVDV2-infected mice. CD8⁺

T lymphocytes in ncp BVDV1-infected mice peaked on day 10 pi, followed by a marked reduction at day 14 pi ($p < 0.05$, Fig. 2b). However, compared with that in ncp BVDV1-infected mice, the count of CD4⁺ T lymphocytes in ncp BVDV2-infected mice increased at day 7 pi, followed by a significant reduction on days 10 ($p < 0.05$) and 14 ($p < 0.01$) (Fig. 2a), while the count of CD8⁺ T lymphocytes did not change much up to day 10 pi and gradually decreased thereafter (Fig. 2b). The CD4⁺ and CD8⁺ T lymphocyte populations expanded more in the spleen of ncp BVDV1-infected animals. In ncp BVDV1-infected mice, the population of B cells increased until day 10 pi ($p < 0.001$) and then decreased at day 14 ($p < 0.05$) (Fig. 2c), whereas in ncp BVDV2-infected mice, the population of B cells increased at day 7 pi and decreased thereafter at day 10 pi ($p < 0.01$) (Fig. 2c). The population of B cells was higher in ncp BVDV1- and ncp BVDV2-infected mice than in mock-infected mice until day 10. As

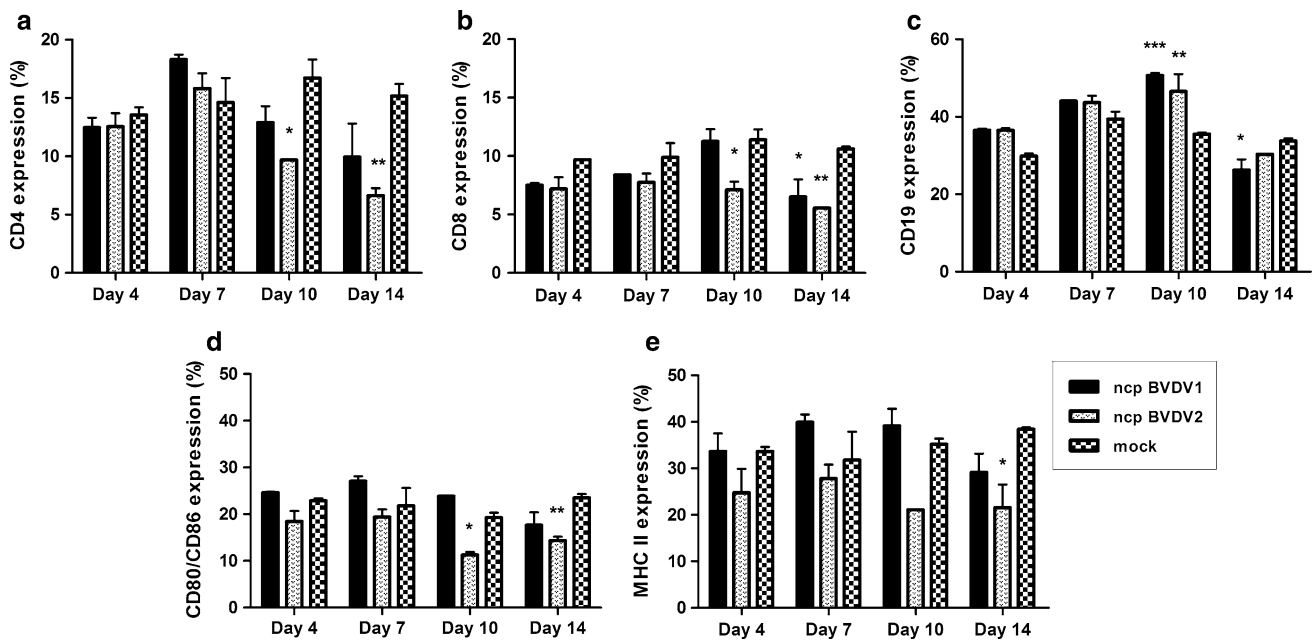


Fig. 2 Splenic cell populations in ncp BVDV1- and ncp BVDV2-infected mice analyzed by flow cytometry for immunophenotyping. Compared with infected ncp BVDV2, ncp BVDV1-infected mice showed increased numbers of CD4⁺ T cells (a), CD8⁺ T cells (b), CD19 (c), CD80 and CD86 (d), and MHC class II (e). Data are

presented as the mean \pm SEM of two independent experiments. Statistical analyses were performed by a two-way analysis of variance (ANOVA), using GraphPad Prism V6.0 software. *, $p < 0.05$; **, $p < 0.01$; and ***, $p < 0.001$ compared with mock-infected group

shown in Fig. 2d and e, the expression of CD80 and CD86, and MHC class II in ncp BVDV2-infected mice on days 4 through 14 pi was lower than that in mock-infected animals, with a significant decline on days 10 ($p < 0.05$, CD80 and CD86) and 14 ($p < 0.01$, CD80 and CD86; $p < 0.05$, MHC II). The expression of CD80, CD86 and MHC class II in ncp BVDV1-infected mice was higher than that in ncp BVDV2-infected mice on days 4 and 10 pi, with a decline at day 14 pi. These results indicate that ncp BVDV2 infection reduces the expression of costimulatory molecules and MHC class II consistently between days 4 and 14.

Quantitative changes in immune cells among splenocytes

To expand upon the changes in immune cells among splenocytes, IHC phenotyping was performed on day 7 pi. Histopathological examination showed lymphoid depletion in the spleens of all BVDV-infected mice from days 4 to 14 (data not shown). The accumulation of B lymphocytes into the follicles of the spleens of both ncp BVDV1- and ncp BVDV2-infected mice was significantly higher than that in the spleens of mock-infected mice. Although most B cells were largely confined to small germinal centers, several B cells were distributed into the splenic sinuses in ncp BVDV1-infected mice (Fig. 3). IHC results showed

that the numbers of CD4⁺ and CD8⁺ T lymphocytes were lower in the spleens of ncp BVDV2-infected mice at day 7 pi compared with those in ncp BVDV1-infected mice (Fig. 4a). To confirm the results of the IHC, the CD4- and CD8-immunostained whole-slide sections were scanned and analyzed with Virtuoso using multiple, manually defined ROI lymphocytes in the center of the spleen at day 7 pi. The positive numbers of CD4⁺ and CD8⁺ T lymphocytes were the highest in mock-infected mice, followed by ncp BVDV1-infected and ncp BVDV2-infected animals (Fig. 4b). In ncp BVDV2-infected mice, the number of the cells that were positive for CD4⁺ decreased significantly at day 7 pi when compared to mock-infected cells ($p < 0.05$). These results of T lymphocyte expression by IHC were consistent with those from the flow cytometric analysis.

ncp BVDV-infected mice induces IL-6 and MCP-1 cytokines

To investigate whether ncp BVDV infection induces proinflammatory responses, we examined several cytokines in the plasma, including IL-6, IL-10, IL-12p70, IFN- γ , TNF- α , and CCL2 (monocyte chemoattractant protein 1 [MCP-1]). As shown in Fig. 5, cytokines/chemokines were either not detected or present at low levels in the plasma of mice infected with both ncp BVDVs. Of the analyzed cytokines/

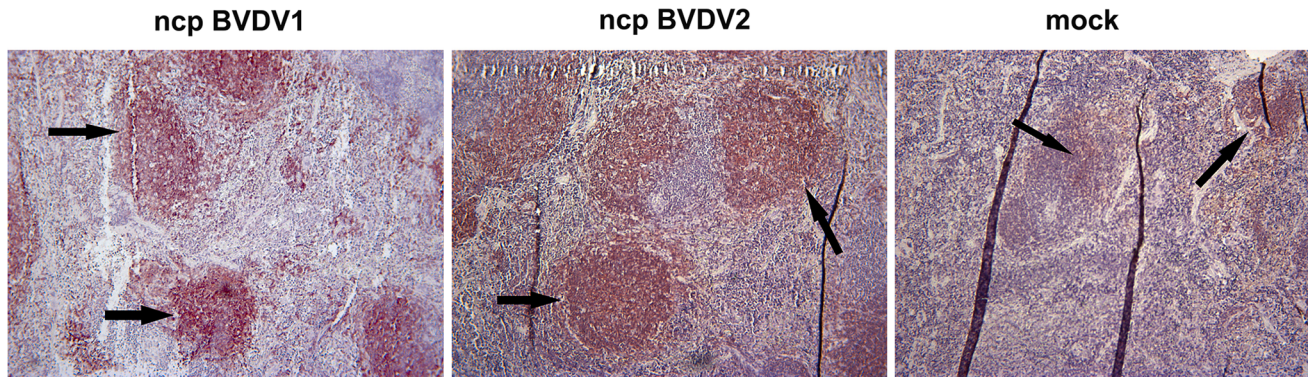
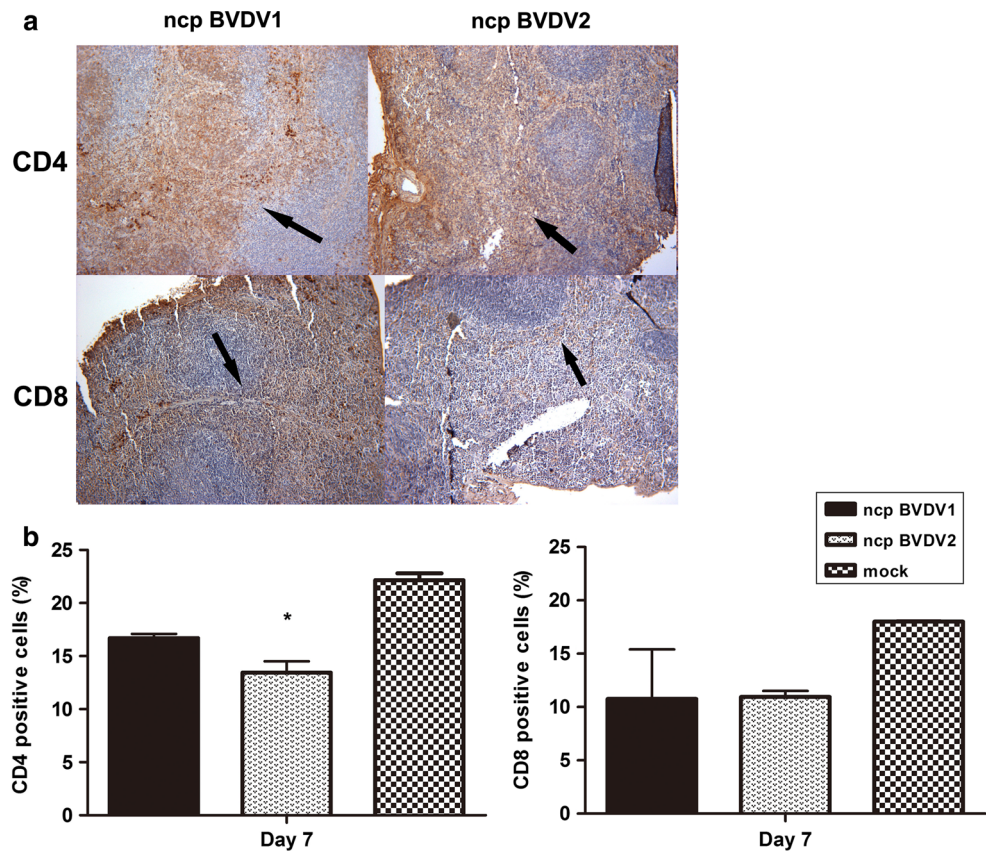


Fig. 3 Immunohistochemical detection of CD45R/B220 B lymphocytes in ncp BVDV1- (left panel), ncp BVDV2- (middle panel), and mock (right panel)-infected mice at day 7 pi. Significant accumulation

of B lymphocytes into the follicles of the spleens was observed in ncp BVDV1-infected mice (arrow; original magnification, 100 \times). The data shown are representative of two repeated experiments

Fig. 4 Immunohistochemical detection of CD4 and CD8 T lymphocytes from ncp BVDV1- (left panels) and ncp BVDV2- (right panels) infected mice at day 7 pi (a). CD4 and CD8 T lymphocytes were largely restricted to follicular germinal centers and paracortex (CD4) and paracortex and medulla (CD8). The population of CD4 and CD8 T lymphocytes was lower in ncp BVDV2-infected mice at day 7 pi. CAIA-based CD4 and CD8 quantification showed reduced numbers of both CD4 and CD8 T lymphocytes in ncp BVDV2-infected mice (b). Data are presented as the mean \pm SEM of two independent experiments. Statistical analyses were performed by a two-way analysis of variance (ANOVA) using GraphPad Prism V6.0 software. A p value less than 0.05 compared to the mock-infected group was considered significant



chemokines, only low levels of IL-6, IL-12, and MCP-1 were detected in both groups, and the other cytokines were not detected. IL-12 was produced only in ncp BVDV1-infected mice at day 4 pi. In addition, mock-infected mice did not produce any cytokines or chemokines. In ncp BVDV2-infected mice, the levels of IL-6 were six times higher than those in ncp BVDV1-infected mice on day 4, with a decline on day 7, and were undetectable thereafter,

whereas IL-6 levels in ncp BVDV1-infected mice were only detected on day 4. The levels of MCP-1 differed between the two groups. In ncp BVDV1-infected animals, MCP-1 was detected only on day 4 and remained undetected from days 7 to 14 pi. In contrast, in ncp BVDV2-infected mice, MCP-1 was detected at day 10, and its level was significantly higher ($p < 0.0001$) than that in ncp BVDV1-infected mice.

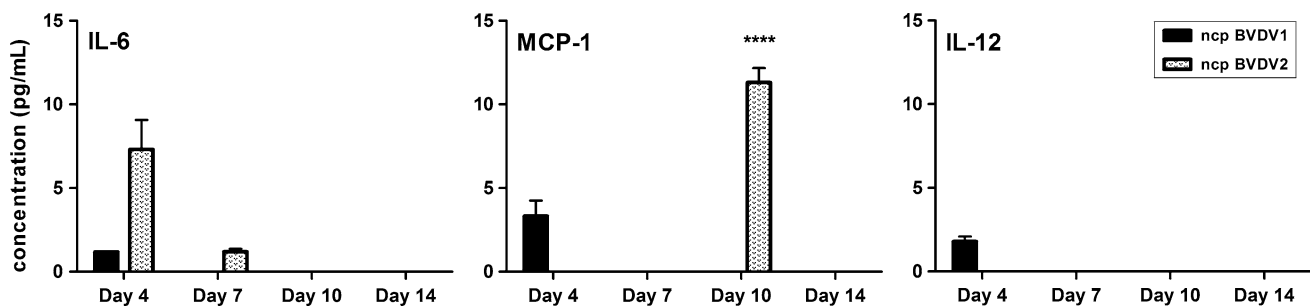


Fig. 5 Analysis of proinflammatory cytokines in the plasma of ncp BVDV1- and ncp BVDV2-infected mice. Data are presented as the mean \pm SEM of two independent experiments. Statistical analyses

were performed by a two-way analysis-of-variance (ANOVA), using GraphPad Prism V6.0 software. ****, $p < 0.0001$ compared with the ncp BVDV1-infected group

Discussion

Interactions between a pathogen and its host control the outcome of an infection. The immunological aspects of such interactions in BVDV infections in mice are not yet understood. In the present study, we showed that ncp BVDV1 and ncp BVDV2 elicit different host cell functions during infection in mice. Interestingly, ncp BVDV2 infection resulted in a decrease in CD4⁺ and CD8⁺ lymphocytes as well as costimulatory (CD80 and CD86) molecules and MHC class II, but ncp BVDV1 did not. Even at low levels, ncp BVDV2 infection induced the production of the proinflammatory cytokines IL-6 and MCP-1. This report presents evidence that ncp BVDV2 has an impact on the host immune system by the negative regulation of immune cell activities. This is the first study to describe the immunopathogenesis of ncp BVDV1 and ncp BVDV2 in a murine model.

In the present study, viral antigens were found in different organs depending on the time of infection (Table 1). Viral antigens were consistently found in the spleen until the end of the experiment. Viral antigens were also detected in the mesenteric lymph nodes, GALT, heart, kidney, intestine, and BALT. Interestingly, viral antigens were detected in the heart, kidney, and intestine at day 4 pi, then not detected at days 7 and 10, and then detected again at day 14 pi. The reason for this is unclear. In natural hosts, viral antigens are widespread in lymphoid tissue and multifocally in intestinal mucosa. Liebler-Tenorio et al. showed that viral antigens were detected in the kidney and the heart of cattle inoculated with a highly virulent ncp BVDV2 strain, suggesting that the highly virulent ncp BVDV2 strain had spread to more organs and tissue types [16]. Therefore, there were significant differences in the detection period and the distribution of viral antigens between natural hosts and mice [15, 16, 20]. The results showed that there are no apparent differences between the target organs used to detect viral antigens between ncp BVDV1 and ncp BVDV2 in the murine model.

Considering that virus was consistently detected in the spleen, our data suggest that the spleen is the most reliable tissue for BVDV antigen detection in a murine model.

Here, we show that ncp BVDV1 infection in mice expanded the CD4⁺ and CD8⁺ T and B cell populations compared to ncp BVDV2 infection. CD4⁺ T cell responses play important roles in enhancing innate immune responses and mediating antiviral effector functions [21–23]. Therefore, the increase in the number of CD4⁺ T cells in ncp BVDV1-infected mice could possibly promote expansion of CD8⁺ T cells and B cells. These observations were confirmed by IHC analysis (Fig. 3 and 4). Unlike those in ncp BVDV1-infected mice, the populations of CD4⁺ and CD8⁺ T cells and B cells significantly decreased in ncp BVDV2-infected animals. Ellis et al. demonstrated that infection of cattle with ncp BVDV1 resulted in transient leucopenia, which was characterized by significant decreases in the absolute numbers of circulating T and B cells [24]. However, the present results showed a reduction in the numbers of these cells in ncp BVDV2 infection. The differences between the two groups might be related to the virus strain used. Ncp BVDV infection induces a CD4⁺ T helper 2 (Th2) response, resulting in high levels of antibodies [25]. CD4⁺ T cells induced in ncp BVDV1 infection lead to the upregulation of MHC class II and costimulatory molecules. This indicates that CD4⁺ T cells may play protective roles via these effects during ncp BVDV1 infection. Therefore, our findings suggest that the increase in the CD4⁺ T cell population after ncp BVDV1 infection might regulate inflammation and directly mediate viral control and clearance, whereas ncp BVDV2 infection might impair the control of the virus in the infected mice. Thus, immunosuppressive effects in BVDV infection may be mediated via CD4⁺ T cells.

The present study indicated that the expression of MHC class II and costimulatory molecules (CD80 and CD86) apparently differs between ncp BVDV1 and ncp BVDV2 infections. The expression of these molecules is required for the generation of an effective immune response. In ncp

BVDV2-infected mice, significant reductions in the levels of these molecules were observed. Similar results have been reported in ncp BVDV2-inoculated calves [13]. Thus, the lack of costimulatory molecules may impair the development of immune responses by inducing T cell anergy or apoptosis instead of activation [26]. The reduction in the expression of MHC class II molecules may hinder the recognition of infected cells by specific T lymphocytes, thus evading some adaptive immune responses [27]. BVDV persists for a long time in infected animals, possible partially due to the ability of the virus to evade the immune recognition system of infected cattle. These results suggest that the critical difference between ncp BVDV1- and ncp BVDV2-infected mice lies at the level of the innate immune response by antigen presentation and costimulatory molecules. Therefore, the reduction of these molecules in ncp BVDV2-infected mice may give some insight into the mechanism leading to the severe clinical signs and immunosuppression observed in natural hosts.

Our results showed that both ncp BVDV infections in mice led to the production of IL-6, MCP-1, and IL-12, although they were secreted at rather low levels. Increased proinflammatory cytokines/chemokines can promote an inflammatory response. Most of all, this increased MCP-1 production in ncp BVDV2-infected mice can influence viral pathogenicity and virulence as well as controlling the spread of infection, resulting in a significant defect in the control of the virus and antiviral effects [28]. IL-12 promotes efficient immune responses against intracellular pathogens. The present results show that IL-12 was either undetected in ncp BVDV2-infected mice or was present at very low levels in ncp BVDV2 infection, indicating that the absence or loss of this cytokine may be closely related to the long-term persistence of an infection. The ncp BVDV shifted the immune response towards the Th2 response and limited the production of high levels of cell-mediated immunity [12]. Previous data demonstrated that TNF α was not produced in ncp BVDV1 and ncp BVDV2 infection, but IFN γ production increased in ncp BVDV1-infected calves [11]. In this study, the production of these cytokines in mice was most likely regulated by CD4⁺ T cells. CD4⁺ T cells are a primary target of BVDV infection and are affected by the biotype and virulence of the virus influencing the signaling and the dynamics of the switch to Th1 or Th2 cells [12]. Further research is needed to clarify this. ncp BVDV2 seems to elicit an inflammatory response with preserved IL-6 and MCP-1 secretion, which may contribute to viral pathogenesis through enhanced virus dissemination.

Collectively, our findings demonstrate that ncp BVDV1 and ncp BVDV2 regulate the host immune response differently. We found that ncp BVDV2 decreases the levels of CD4⁺ and CD8⁺ T lymphocytes, B lymphocytes, antigen

presentation, and costimulatory molecules and induces proinflammatory cytokines. This suggests that ncp BVDV2 fails to control and clear the virus in the animals, resulting in defective antigen presentation and costimulatory signals, enhanced virus dissemination, and severe immunosuppression in natural hosts. These results provide insights into the immunopathogenesis of ncp BVDV1 and ncp BVDV2 infection in mice.

Acknowledgments This work was supported by the Basic Science Research Program of the National Research Foundation of Korea, funded by the Ministry of Education, Science, and Technology (NRF 2012R1A1A3011238).

References

- Baker JC (1995) The clinical manifestations of bovine viral diarrhea infection. *Vet Clin N Am Food Anim Pract* 11:425–445
- Ridpath JF, Bendfeldt S, Neill JD, Liebler-Tenorio E (2006) Lymphocytopenic activity in vitro correlates with high virulence in vivo for BVDV type 2 strains: criteria for a third biotype of BVDV. *Virus Res* 118:62–69
- Deregt D, Loewen KG (1995) Bovine viral diarrhea virus: biotypes and disease. *Can Vet J* 36:371–378
- Dubovi EJ (1994) Impact of bovine viral diarrhea virus on reproductive performance in cattle. *Vet Clin N Am Food Anim Pract* 10:503–514
- Brownlie J, Clarke MC, Howard CJ (1984) Experimental production of fatal mucosal disease in cattle. *Vet Rec* 114:535–536
- Hamers C, Couvreur B, Dehan P, Letellier C, Lewalle P, Pastoret PP, Kerkhofs P (2000) Differences in experimental virulence of bovine viral diarrhoea viral strains isolated from haemorrhagic syndromes. *Vet J* 160:250–258
- Kelling CL, Topliff CL (2013) Bovine maternal, fetal and neonatal responses to bovine viral diarrhea virus infections. *Biologicals* 41:20–25
- Ridpath JF, Neill JD, Peterhans E (2007) Impact of variation in acute virulence of BVDV1 strains on design of better vaccine efficacy challenge models. *Vaccine* 25:8058–8066
- Potgieter LN (1995) Immunology of bovine viral diarrhea virus. *Vet Clin N Am Food Anim Pract* 11(3):501–520
- Wood RD, Goens SD, Carman PS, Deregt D, Jefferson B, Jacobs RM (2004) Effect on hematopoietic tissue of experimental infection of calves with noncytopathic type 2 bovine viral diarrhea virus. *Can J Vet Res* 68:42–48
- Seong G, Oem JK, Choi KS (2013) Pathogenetic differences after experimental infection of calves with Korean non-cytopathic BVDV-1 and BVDV-2 isolates. *Vet Immunol Immunopathol* 156:147–152
- Chase CC (2013) The impact of BVDV infection on adaptive immunity. *Biologicals* 41:52–60
- Archambault D, Béliveau C, Couture Y, Carman S (2000) Clinical response and immunomodulation following experimental challenge of calves with type 2 noncytopathogenic bovine viral diarrhea virus. *Vet Res* 31:215–227
- Lee SR, Pharr GT, Boyd BL, Pinchuk LM (2008) Bovine viral diarrhea viruses modulate toll-like receptors, cytokines and costimulatory molecules genes expression in bovine peripheral blood monocytes. *Comp Immunol Microbiol Infect Dis* 31:403–418
- Liebler-Tenorio EM, Ridpath JE, Neill JD (2002) Distribution of viral antigen and development of lesions after experimental

- infection with highly virulent bovine viral diarrhoea virus type 2 in calves. *Am J Vet Res* 63:1575–1584
16. Liebler-Tenorio EM, Ridpath JF, Neill JD (2003) Distribution of viral antigen and development of lesions after experimental infection of calves with a BVDV 2 strain of low virulence. *J Vet Diagn Invest* 15:221–232
 17. Seong G, Oem JK, Lee KH, Choi KS (2015) Experimental infection of mice with bovine viral diarrhoea virus. *Arch Virol* 160:1565–1571
 18. Seong G, Lee JS, Lee KH, Choi KS (2015) Experimental infection with cytopathic bovine viral diarrhoea virus in mice induces megakaryopoiesis in the spleen and bone marrow. *Arch Virol*. doi:10.1007/s00705-015-2649-y
 19. Reed LJ, Muench H (1938) A simple method of estimating fifty percent endpoints. *Am J Hyg* 27:493–497
 20. Liebler-Tenorio EM, Ridpath JF, Neill JD (2003) Lesions and tissue distribution of viral antigen in severe acute versus sub-clinical acute infection with BVDV2. *Biologicals* 31:119–122
 21. Clouthier DL, Zhou AC, Wortzman ME, Luft O, Levy GA, Watts TH (2015) GITR intrinsically sustains early type 1 and late follicular helper CD4 T cell accumulation to control a chronic viral infection. *PLoS Pathog* 11:e1004517
 22. Soriano-Sarabia N, Bateson RE, Dahl NP, Crooks AM, Kuruc JD, Margolis DM, Archin NM (2014) Quantitation of replication-competent HIV-1 in populations of resting CD4⁺ T cells. *J Virol* 88:14070–14077
 23. Swain SL, McKinstry KK, Strutt TM (2012) Expanding roles for CD4⁺ T cells in immunity to viruses. *Nat Rev Immunol* 12:136–148
 24. Ellis JA, Davis WC, Belden EL, Pratt DL (1988) Flow cytometric analysis of lymphocyte subset alterations in cattle infected with bovine viral diarrhoea virus. *Vet Pathol* 25:231–236
 25. Rhodes SG, Cocksedge JM, Collins RA, Morrison WI (1999) Differential cytokine responses of CD4⁺ and CD8⁺ T cells in response to bovine viral diarrhoea virus in cattle. *J Gen Virol* 80:1673–1679
 26. Rodríguez-Calvo T, Rojas JM, Martín V, Sevilla N (2014) Type I interferon limits the capacity of bluetongue virus to infect hematopoietic precursors and dendritic cells in vitro and in vivo. *J Virol* 88:859–867
 27. Ferrero MC, Hielpos MS, Carvalho NB, Barrionuevo P, Corsetti PP, Giambartolomei GH, Oliveira SC, Baldi PC (2014) Key role of Toll-like receptor 2 in the inflammatory response and major histocompatibility complex class ii downregulation in *Brucella abortus*-infected alveolar macrophages. *Infect Immun* 82:626–639
 28. Zhao G, Liu C, Kou Z, Gao T, Pan T, Wu X, Yu H, Guo Y, Zeng Y, Du L, Jiang S, Sun S, Zhou Y (2014) Differences in the pathogenicity and inflammatory responses induced by avian influenza A/H7N9 virus infection in BALB/c and C57BL/6 mouse models. *PLoS One* 9:e92987